Journal of Neurology & Neurophysiology

Inaki et al., J Neurol Neurophysiol 2016, 7:1
DOI: 10.4172/2155-9562.1000351

Research Article Open Access

Altered Regional CBF Correlates with Repeatable Battery for the Assessment of Neuropsychological Status (RBANS) Profile in the Patients with Memory Lapse

Anri Inaki[1*], Nozomi Funaki[2], Tetsumori Yamashima[2], Hiroshi Wakabayashi[1], Junichi Taki[1], Yoshio Minabe[3] and Seigo Kinuya[1]

[1]*Department of Nuclear Medicine, Kanazawa University Hospital, Kanazawa, Japan*

[2]*Department of Restorative Neurosurgery, Kanazawa University Hospital, Kanazawa, Japan*

[3]*Department of Psychiatry and Neurobiology, Graduate School of Medical Science, Kanazawa, University, Kanazawa, Japan*

***Corresponding author:** Anri Inaki, Department of Nuclear Medicine, Kanazawa University Hospital, Kanazawa, 13-1 Takara-machi, Kanazawa, Japan, Tel: +81-76-265-2333; Fax: +81-76-234-4257; E-mail: henri@nmd.m.kanazawa-u.ac.jp

Received date: December 22, 2015; **Accepted date:** January 20, 2016; **Published date:** January 27, 2016

Abstract

Repeatable Battery for the Assessment of Neuropsychological Status (RBANS) has been used for the detection of Alzheimer's disease, because its diagnostic value is not widely accepted due to lack of supportive imaging data. In this study, we retrospectively evaluated the validity of RBANS by single photon emission computed tomography (SPECT) to evaluate regional cerebral blood flow (rCBF). Methods: We enrolled 87 subjects with complaints of memory impairment who underwent both RBANS and SPECT. The RBANS scores were assessed, correlating with the decrease of rCBF in the crucial areas. Results: Linear regression analysis showed a significant positive correlation between the total and delayed memory scores of RBANS and the rCBF of the posterior cingulate gyrus and the precuneus. In the 2-sample t-test, the rCBF of the posterior cingulate gyrus in the patients with a total RBANS score of less than 34 was significantly lower, compared to those with a score more than 35. Conclusion: These data indicated a significant correlation between the RBANS total score and the perfusion of the posterior cingulate gyrus, and both methods are considered complementarily useful for detecting early Alzheimer's disease.

Keywords: Cognitive impairment; RBANS; Neuropsychological test; Scintigraphy; Regional CBF

Introduction

Alzheimer's disease (AD) is the most common disease of dementia, which slowly causes progressive cognitive impairment and eventually leads to complete loss of behavior. Although some researches have advocated several hypotheses about the etiology of AD (e.g. the amyloid hypothesis, the tau hypothesis, implications of cerebral ischemia, type 2 diabetes, or brain trauma etc.) [1], they are yet conclusive. Because of the absence of a complete cure or prophylaxis of AD, current anti-Alzheimer therapy has mainly focused on delaying its progression, and anti-Alzheimer's agents can impede the progression of AD only by early intervention [2]. Accordingly, one of the most important standpoints for treatment of AD is to diagnose it at an earlier stage. A combination of neuropsychological tests and brain imaging modalities is generally accepted to be a standard method for the diagnosis of AD.

There are a variety of neuropsychological examinations, for example: [1] the mini-mental state examination (MMSE) as a brief screening test, [2] the Alzheimer's Disease Assessment Scale-cognitive subscale (ADAS-cog), and [3] the Wechsler Memory Scale-Revised (WMS-R) as comprehensive neuropsychological batteries. Although the MMSE has been widely utilized due to its simplicity in the clinical practice, such simple test batteries can hardly assess extent of memory deficits in detail. On the other hand, the ADAS-cog and the WMS-R can evaluate several items (e.g. auditory memory and immediate memory) semi-quantitatively in lieu of their complexity.

However, these neuropsychological tests are troublesome for both the patients and doctors in the outpatient clinics. Furthermore, diagnosis of early AD is not easy, because the assessment of recent memory and/or concentration (attention) impairments is imprecise in these test batteries.

Repeatable Battery for the Assessment of Neuropsychological Status (RBANS) is a test battery utilized worldwide for detecting cognitive deficits in the clinical practice [3]. It consists of 1 total score and 5 sub-scores, each of which can quantitate functions of immediate memory, delayed memory, attention, language, and visuospatial/constructional skills. One battery takes less than 30 minutes for examination and 10 minutes for scoring, which leads to ease of implementation. Previous studies have reported usefulness of RBANS for detecting early AD [4-6] and mild cognitive impairment [7,8].

The aim of this study was to correlate the RBANS data with single photon emission computed tomography (SPECT) data, and to confirm the usefulness of the RBANS combined with SPECT for the diagnosis of early AD.

Materials and Methods

Patient inclusion and exclusion criteria

The present study was approved by the ethics committee of both Kanazawa University Hospital and Minamigaoka Hospital. We enrolled 87 patients who had complained of memory impairment and consulted the out-patient clinic of the latter hospital. We informed all patients of the details of this study and are permitted to use their data in this study. All subjects underwent the RBANS and SPECT, the

procedures of which are shown below. Additionally, we also performed Magnetic Resonance Imaging (MRI) on all subjects and excluded any organic brain diseases such as cerebral infarction, hemorrhage, contusions or anomalies.

Neuropsychological tests

In this study, we used the Japanese version of the RBANS, which has been translated into Japanese, and standardized by Yamashima et al. [9]. Details of the Japanese version were described in the previous paper [3]. Briefly, it consists of 1 total score and 5 sub-scores which were yielded by 12 raw scores. With the age-based correction, raw scores were converted to sub-scores including immediate memory (IM), visuospatial/constructional (VC), language, attention, and delayed recall of memory (DM).

Imaging and image analyses

All SPECT studies were done at the Kanazawa University Hospital, using an e.cam signature dual-headed gamma camera (Siemens Medical Solutions USA Inc., Pennsylvania, USA) that was equipped with low-energy high-resolution parallel-hole collimators. Each patient received an intravenous injection of 740MBq of 99mTc-labelled ethyl cysteinate dimer (99mTc-ECD) (FUJIFILM RI Pharma Co. Ltd., Tokyo, Japan), and 10 minutes after the injection brain SPECT was performed for 20 minutes. After applying a Butterworth filter (cut-off frequency=0.65 cycle/cm, order=8) as a smoothing filter, SPECT images were reconstructed from projection images by the filtered back projection (FBP) algorithm using a ramp filter with 6 mm in full width at half maximum (FWHM). Scatter correction and attenuation correction were performed according to the triple energy window (TEW) method and Chang's method, respectively.

The SPECT images were executed by Statistical Parametric Mapping 8 (SPM8) (Wellcome Department of Imaging Neuroscience, London, UK) running on MATLAB 2013a (Mathworks, Inc., Massachusetts, USA), which performed voxel-based analysis for comparison of these images. All images were spatially normalized into the Montreal Neurological Institute (MNI) space and smoothed with a gaussian kernel with 12 mm in FWHM.

Statistics

The processed images were also analyzed by SPM8. First, we calculated voxel-based correlation analysis between the SPECT images and the RBANS scores; the linear regression analysis was performed between each voxel and an arbitrary value. In order to detect the cut-off value of the RBANS total score, we divided the subjects in 2 groups by setting cut-off values of the RBANS total score at 30, 35, 40, 45 or 50 to calculate the extent of a region of each subject. Details of this method were already described by Matsuda et al. [10]. Briefly, this indicator means the percent rate of the coordinates where the rCBF decreases significantly. Then, we estimated area under the curve (AUC) in receiver operating characteristic (ROC) curve of each classification. ROC curve is a graphical plot created on a two-dimensional coordinate system by plotting the fraction of true positive rate versus that of false positive rate. Second, in accordance with the optimized cut-off value, we performed statistical analysis of patients' characteristics and voxel-based analysis with Mann-Whitney's U-test and two-sample t-test between groups, respectively.

SPM8 was used for each image analysis, in which age, sex and year of education were included as nuisance covariates. The resulting sets of t values were transformed to the unit normal distribution (Z-score) and projected onto the three-dimensional rendered brain provided by SPM8 with a threshold of $p<0.001$ (uncorrected). We used the WFU pickatlas (the Advanced Neuroscience Imaging Research lab, North Carolina, USA) for the identification of statistically significant areas in the MNI coordinates [11,12]. Statistical analysis, except for the image analysis, was performed using a statistical software package JMP® (SAS Institute Inc., North Carolina, USA).

Results

No correlation was found between the RBANS scores and age, sex and year of education.

Result of the voxel-based correlation analysis between the SPECT images and the RBANS scores was shown in Figure 1. The red area shows a low perfusion area that significantly correlated with the decrease of each score on the RBANS. Cluster-level analysis showed that the total and the DM scores correlate significantly with the rCBF in the bilateral posterior cingulate gyri and precunei, with a peak of the left precuneus (-4 -62 32 and -6 -60 32, x y z in the MNI space, respectively). In the peak-level analysis, a significant correlation was found between the attention score and the right cuneus (8 -78 8, x y z), the language score and the left declive (-26 -54 -16, x y z), as well as the VC score and the right hippocampal gyrus (26 -56 2, x y z), respectively. No significant decline of rCBF was found in relation to IM score.

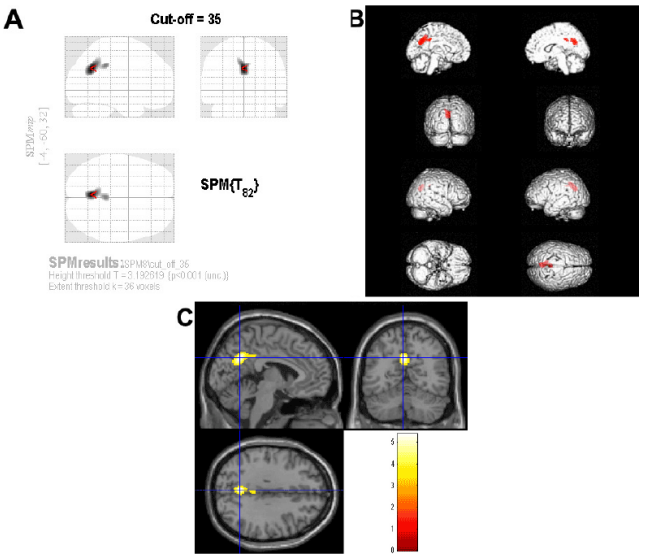

Figure 1: Linear regression analysis between the RBANS scores and the rCBF SPECT. The results were projected on the standard MRI templates provided by SPM8 and arranged from top to bottom: medial left, medial right, lateral right, lateral left, anterior, posterior, top and bottom views. The red areas indicated a significantly low perfusion with the decrease of each of the RBANS scores described below. DM=Delayed Memory; IM=Immediate Memory; VC=Visuospatial/Constructional skills.

The ROC analysis for detecting rCBF abnormality with various thresholds of the RBANS total score was shown in Figure 2. Among the five cut-off points (30, 35, 40, 45 and 50) studied, the score of 35

showed the highest value of AUC (0.728). Accordingly, we divided the patients into 2 groups: patients with the RBANS scores 35 or more and patients with those less than 35. Between the 2 groups of patients, no significant difference in age, sex, and years of disease duration was found, however, each of the five sub-scores of the patients whose total score was 35 and more was significantly higher than those of the patients whose total score was less than 35 (Table 1).

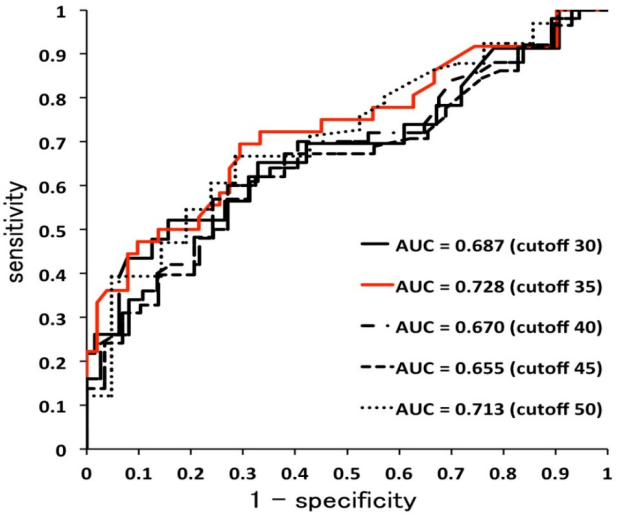

Figure 2: Receiver operating characteristics (ROC) curve for the score of the extent of the decreased area. This indicator means the percent rate of the coordinates where the rCBF decreases significantly in the region correlating RBANS total score. The highest accuracy was seen by setting a threshold at 35 (red line). AUC=Area Under the Curve.

	RBANS Total Score		p value*
	>35	≤ 35	
age	64.6 ± 9.3	65.9 ± 11.3	n.s.
sex (F/M)	28/23	16/20	n.s.
year of education	12.8 ± 3.0	11.2 ± 2.5	n.s.
RBANS sub-scores			
Attention	49.9 ± 11.1	37.2 ± 9.7	<0.0001
Delayed Memory	49.0 ± 12.0	35.3 ± 12.4	<0.0001
Immediate Memory	51.7 ± 10.6	38.0 ± 8.5	<0.0001
Language	48.6 ± 9.0	41.2 ± 7.3	<0.0001
Visuospatial	53.3 ± 9.0	46.1 ± 13.1	0.0034

Table 1: Patients' Demography (*Mann-Whitney's U-test).

Two-sample t test indicated a significant correlation between the RBANS total score and the rCBF in the bilateral posterior cingulate gyri and precunei with a peak of the left precuneus (-4 -60 32, x y z) by setting the cut-off value at 35 (Figure 3).

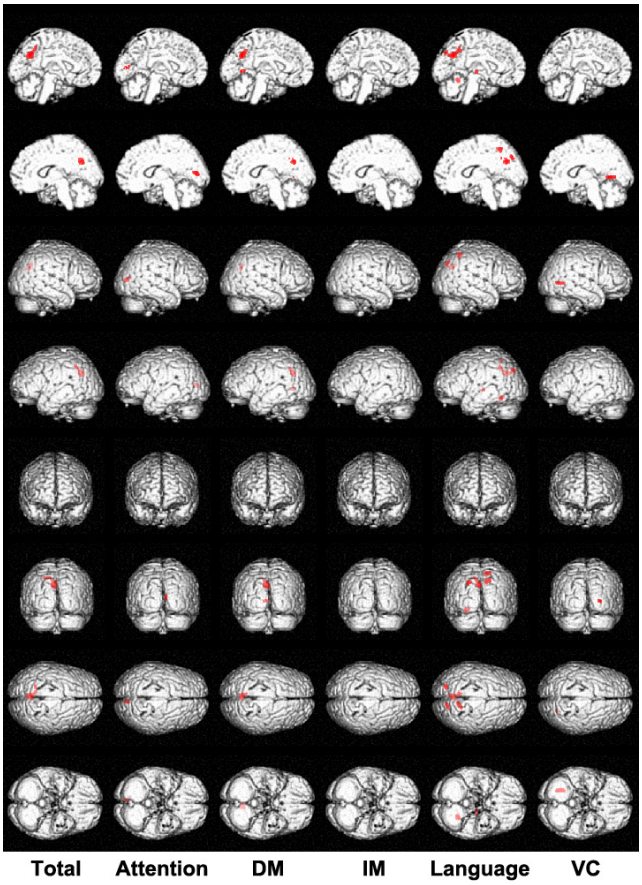

Figure 3: Two-sample t-test between the patients with the RBANS score ≥ 35 and the patients with the RBANS score <35. A significant low-perfusion of the bilateral posterior cingulate gyri and precuneus was found in patients with the RBANS score <35. (A) and (B) Maximum intensity projection thresholded with p<0.001 (uncorrected). (C) Color-scaled Z-score map overlaid on the standard MR templates provided by SPM8.

Discussion

In this study, we first evaluated effectiveness of the RBANS combined with SPECT imaging for the diagnosis of early AD. Intriguingly, the present data indicated a significant correlation between the RBANS total score and the perfusion of the PCC. This suggested that the RBANS combined with SPECT may be useful to detect early AD. The hypo-perfusion in the bilateral PCC and precunei were already confirmed in the early AD patients by the previous studies [10,13]. Another study also reported that rCBF SPECT could discriminate between the conversion group and the non-conversion group from MCI to AD [14]. It is suggested from these reports that RBANS can distinguish early AD patients from healthy subjects.

For the last two decades, nuclear neuroimaging approaches such as PET and SPECT have been utilized for the diagnosis of early AD in the clinical practice. Although many studies have reported the usefulness of an in-vivo biomarker 11C-PiB for amyloid β imaging on PET, it is still not widely used, because of the necessity of exclusive facilities (e.g.

cyclotron) to generate 11C-PiB. The more conventional methodology for the diagnosis of AD is 18F-fludeoxyglucose PET (FDG-PET) to detect glucose hypo-metabolism and SPECT to detect decrease of the regional cerebral blood flow (rCBF). However, the probable diagnosis of early AD is not always achievable only through these methods of neuroimaging. Accordingly, appropriate neuropsychological examinations or certain biomarkers combined with these neuroimaging modalities may be preferable for the diagnosis of early AD.

Research criteria revised from the NINCDS-ADRDA Alzheimer's Criteria enumerating supportive features of probable AD included medial temporal lobe atrophy, abnormal cerebrospinal fluid (CSF) biomarker, and specific pattern on functional neuroimaging with PET [15]. Since Motter et al. and Arai et al. had reported a specific reduction of amyloid β-42 [16] and increase of Tau protein in the CSF [17], respectively, the following studies confirmed usefulness of several CSF biomarkers [18,19]. Thereafter, many studies confirmed the usefulness of the CSF biomarkers, not only for detecting early AD, but also for predicting future progression from MCI to AD. However, although these techniques were supposed to improve accuracy of the diagnosis of AD, sampling of the CSF as a screening tool is invasive to both the healthy and early AD subjects.

On the other hand, less-invasive functional neuroimaging with PET, for detecting glucose hypo-metabolism in the specific region on FDG-PET and deposition of amyloid β-42 on 11C-PiB PET, has recently been focused in the clinical practice [20]. In addition, Hashimoto et al. recently succeeded in the novel Tau imaging, which is much more parallel to the severity of AD [21] than amyloid PET. For the past 2 decades, many researchers have demonstrated the usefulness of rCBF SPECT and 18F-FDG PET for the detection of AD and its progression. In particular, since Minoshima et al. reported metabolic reduction of the posterior cingulate cortex (PCC) by FDG-PET in early AD patients [22,23], and moreover, since the decreased rCBF of this area was also confirmed on SPECT [10,13], these modalities have been approved for detecting early AD.

Neuropsychological examination is non-invasive and appropriate for the screening of early AD patients, if the screening of memory and/or concentration (attention) is done properly and precisely. Since the proposal of RBANS by Randolph et al. [3], it has been used by many investigators for the assessment of cognitive dysfunctions. Although the RBANS initially focused on detecting and characterizing schizophrenia, it has also been applied to various diseases that cause cognitive impairments. With respect to the relationship between the RBANS and neuroimaging examinations, Forsters et al. demonstrated a significant correlation between the score of the RBANS figure copy test and FDG uptake in the bilateral fusiform gyri, the right inferior temporal gyrus, the left anterior cingulate gyrus, the left parahippocampal gyrus, the right middle temporal gyrus, and the right insula in patients with Alzheimer's disease [24]. However, the correlation between the neuroimaging data and the RBANS profiles focusing on early AD was not found until now.

The PCC is considered to pertain to many neuropsychological disorders [25], because of the connection with the default mode network (DMN) [26,27]. The DMN is known to be deactivated under neuropsychological tasks and, conversely, activated during internal mentation away from external stimuli, namely stimulus-independent thoughts [28]. Another study reported increased activity of the PCC during recall from autobiographical memory [29]. Current theories suggest that the PCC plays a crucial role in the DMN affecting mental activity such as attention, arousal, and thought, which may cause several symptoms of AD.

Conclusion

We compared the RBANS score with perfusion SPECT in patients with memory impairments in order to investigate the usefulness of the RBANS. The present results showed a significant correlation between the RBANS total score and the perfusion of the PCC. It is suggested that combination of these data may be useful for detecting early Alzheimer's disease.

References

1. Jack CR, Holtzman DM (2013) Biomarker modeling of Alzheimer's disease. Neuron 80: 1347-1358.
2. Galluzzi KE, Appelt DM, Balin BJ (2010) Modern care for patients with Alzheimer disease: rationale for early intervention. J Am Osteopath Assoc 110: S37-42.
3. Randolph C, Tierney MC, Mohr E, Chase TN (1998) The Repeatable Battery for the Assessment of Neuropsychological Status (RBANS): preliminary clinical validity. J Clin Exp Neuropsychol 20: 310-319.
4. Holzer L, Chinet L, Jaugey L, Plancherel B, Sofia C, et al. (2007) Detection of cognitive impairment with the Repeatable Battery for the Assessment of Neuropsychological Status (RBANS) in adolescents with psychotic symptomatology. Schizophr Res 95: 48-53.
5. Duff K, Humphreys Clark JD, O'Bryant SE, Mold JW, Schiffer RB, et al. (2008) Utility of the RBANS in detecting cognitive impairment associated with Alzheimer's disease: sensitivity, specificity, and positive and negative predictive powers. Arch Clin Neuropsychol 23: 603-612.
6. Karantzoulis S, Novitski J, Gold M, Randolph C (2013) The Repeatable Battery for the Assessment of Neuropsychological Status (RBANS): Utility in detection and characterization of mild cognitive impairment due to Alzheimer's disease. Arch Clin Neuropsychol 28: 837-844.
7. Phillips R, Qi G, Collinson SL (2015) The Minimum Clinically Important Difference in the Repeatable Battery for the Assessment of Neuropsychological Status. Clin Neuropsychol .
8. Fyock CA, Hampstead BM (2015) Comparing the relationship between subjective memory complaints, objective memory performance, and medial temporal lobe volumes in patients with mild cognitive impairment. Alzheimers Dement (Amst) 1: 242-248.
9. Yamashima T, Yoshida M, Kumahashi K, Matsui M, Koshino Y, et al. (2002) [The Japanese version of RBANS (Repeatable Battery for the Assessment of Neuropsychological Status)]. No To Shinkei 54: 463-471.
10. Matsuda H, Mizumura S, Nagao T, Ota T, Iizuka T, et al. (2007) Automated discrimination between very early Alzheimer disease and controls using an easy Z-score imaging system for multicenter brain perfusion single-photon emission tomography. AJNR Am J Neuroradiol 28: 731-736.
11. Lancaster JL, Rainey LH, Summerlin JL, Freitas CS, Fox PT, et al. (1997) Automated labeling of the human brain: a preliminary report on the development and evaluation of a forward-transform method. Hum Brain Mapp 5: 238-242.
12. Lancaster JL, Woldorff MG, Parsons LM, Liotti M, Freitas CS, et al. (2000) Automated Talairach atlas labels for functional brain mapping. Hum Brain Mapp 10: 120-131.
13. Kogure D, Matsuda H, Ohnishi T, Kunihiro T, Uno M, et al. (1999) [Longitudinal evaluation of early dementia of Alzheimer type using brain perfusion SPECT]. Kaku Igaku 36: 91-101.
14. Devanand DP, Van Heertum RL, Kegeles LS, Liu X, Jin ZH, et al. (2010) (99m)Tc hexamethyl-propylene-aminoxime single-photon emission computed tomography prediction of conversion from mild cognitive impairment to Alzheimer disease. Am J Geriatr Psychiatry 18: 959-972.

15. Dubois B, Feldman HH, Jacova C, Dekosky ST, Barberger-Gateau P, et al. (2007) Research criteria for the diagnosis of Alzheimer's disease: revising the NINCDS-ADRDA criteria. Lancet Neurol 6: 734-746.
16. Motter R, Vigo-Pelfrey C, Kholodenko D, Barbour R, Johnson-Wood K, et al. (1995) Reduction of beta-amyloid peptide42 in the cerebrospinal fluid of patients with Alzheimer's disease. Ann Neurol 38: 643-648.
17. Arai H, Terajima M, Miura M, Higuchi S, Muramatsu T, et al. (1995) Tau in cerebrospinal fluid: a potential diagnostic marker in Alzheimer's disease. Ann Neurol 38: 649-652.
18. Morinaga A, Ono K, Ikeda T, Ikeda Y, Shima K, et al. (2010) A comparison of the diagnostic sensitivity of MRI, CBF-SPECT, FDG-PET and cerebrospinal fluid biomarkers for detecting Alzheimer's disease in a memory clinic. Dementia and geriatric cognitive disorders 30: 285-292.
19. Weih M, Degirmenci U, Kreil S, Suttner G, Schmidt D, et al. (2011) Nuclear medicine diagnostic techniques in the era of pathophysiology-based CSF biomarkers for Alzheimer's disease. J Alzheimers Dis 26 Suppl 3: 97-103.
20. Bloudek LM, Spackman DE, Blankenburg M, Sullivan SD (2011) Review and meta-analysis of biomarkers and diagnostic imaging in Alzheimer's disease. J Alzheimers Dis 26: 627-645.
21. Hashimoto H, Kawamura K, Igarashi N, Takei M, Fujishiro T, et al. (2014) Radiosynthesis, Photoisomerization, Biodistribution, and Metabolite Analysis of 11C-PBB3 as a Clinically Useful PET Probe for Imaging of Tau Pathology. J Nucl Med 55: 1532-1538.
22. Minoshima S, Foster NL, Kuhl DE (1994) Posterior cingulate cortex in Alzheimer's disease. Lancet 344: 895.
23. Minoshima S, Giordani B, Berent S, Frey KA, Foster NL, et al. (1997) Metabolic reduction in the posterior cingulate cortex in very early Alzheimer's disease. Ann Neurol 42: 85-94.
24. Förster S, Teipel S, Zach C, Rominger A, Cumming P, et al. (2010) FDG-PET mapping the brain substrates of visuo-constructive processing in Alzheimer's disease. J Psychiatr Res 44: 462-469.
25. Leech R, Sharp DJ (2014) The role of the posterior cingulate cortex in cognition and disease. Brain 137: 12-32.
26. Raichle ME, MacLeod AM, Snyder AZ, Powers WJ, Gusnard DA, et al. (2001) A default mode of brain function. Proc Natl Acad Sci U S A 98: 676-682.
27. Buckner RL, Andrews-Hanna JR, Schacter DL (2008) The brain's default network: anatomy, function, and relevance to disease. Ann N Y Acad Sci 1124: 1-38.
28. Mason MF, Norton MI, Van Horn JD, Wegner DM, Grafton ST, et al. (2007) Wandering minds: the default network and stimulus-independent thought. Science 315: 393-395.
29. Svoboda E, McKinnon MC, Levine B (2006) The functional neuroanatomy of autobiographical memory: a meta-analysis. Neuropsychologia 44: 2189-2208.